

An overview of measurement comparisons from the INTEX-B/MILAGRO airborne field campaign

M. M. Kleb¹, G. Chen¹, J. H. Crawford¹, F. M. Flocke², and C. C. Brown^{1,3}

¹NASA Langley Research Center, Hampton, Virginia, USA

²National Center for Atmospheric Research, Boulder, Colorado, USA

³Science Systems and Applications, Inc., Hampton, Virginia, USA

Received: 22 April 2010 – Published in Atmos. Meas. Tech. Discuss.: 18 May 2010

Revised: 18 November 2010 – Accepted: 21 November 2010 – Published: 11 January 2011

Abstract. As part of the NASA's INTEX-B mission, the NASA DC-8 and NSF C-130 conducted three wing-tip to wing-tip comparison flights. The intercomparison flights sampled a variety of atmospheric conditions (polluted urban, non-polluted, marine boundary layer, clean and polluted free troposphere). These comparisons form a basis to establish data consistency, but also should also be viewed as a continuation of efforts aiming to better understand and reduce measurement differences as identified in earlier field intercomparison exercises. This paper provides a comprehensive overview of 140 intercomparisons of data collected as well as a record of the measurement consistency demonstrated during INTEX-B. It is the primary goal to provide necessary information for the future research to determine if the observations from different INTEX-B platforms/instrument are consistent within the PI reported uncertainties and used in integrated analysis. This paper may also contribute to the formulation strategy for future instrument developments. For interpretation and most effective use of these results, the reader is strongly urged to consult with the instrument principle investigator.

1 Introduction

The Intercontinental Chemical Transport Experiment-B (INTEX-B) was the second major airborne field mission conducted in the spring of 2006 as part of the NASA-led INTEX-NA (North America) mission, aiming to investigate the transport and transformation of pollution over the North American continent. INTEX-B operated in coordination with a larger program, the MILAGRO (Mega-city Initiative: Local and Global Research Observations) and IMPEX (Inter-

continental and Mega-city Pollution Experiment) missions. INTEX-B was comprised of two phases. Phase one occurred from 1–21 March to maximize overlap with the MILAGRO campaign. During this phase, observations were primarily over Mexico and the Gulf of Mexico. The second phase lasted from 15 April to 15 May and focused on Asian pollution transported across the Pacific Ocean. Five specific goals were identified for INTEX-B: (1) to investigate the extent and persistence of the outflow of pollution from Mexico; (2) to understand the transport and evolution of Asian pollution, the related air quality, and climate implications in western North America; (3) to relate atmospheric composition to chemical sources and sinks; (4) to characterize the effects of aerosols on radiation; and (5) to validate satellite observations of tropospheric composition (Singh et al., 2009). For a complete mission overview, reader is referred to Singh et al. (2009).

The INTEX-B field mission involved two comparably equipped aircraft, the NASA DC-8 and NSF C-130. The sampling strategy often required coordination of both aircraft while making measurements in different regions or times. This naturally led to the pre-planning and execution of a series of comprehensive measurement comparisons of species/parameters measured on both platforms. The overarching goal was to generate a program-wide unified data set from all available resources to better address the science objectives. These comparisons form a basis to establish data consistency. The INTEX-B measurement comparison exercise should also be viewed as a continuation of efforts aiming to better understand and reduce measurement differences as identified in earlier field intercomparison exercises (e.g. NASA TRACE-P, Eisele et al., 2003; and ICARTT, <http://www-air.larc.nasa.gov/missions/intexna/meas-comparison.htm>). It is recognized that further comparisons of the in-situ data sets to satellite retrievals, lidar, and model output are equally important; however such analyses are beyond the scope of this paper.



Correspondence to: M. M. Kleb
(mary.m.kleb@nasa.gov)

2 Background

NASA has a long history of conducting instrument intercomparisons beginning with ground-based intercomparisons in July 1983 (Hoell et al., 1984, 1985a,b; Gregory et al., 1985) prior to the commencement of the airborne field studies in October 1983 with the Chemical Instrumentation Test and Evaluation (CITE) missions (Beck et al., 1987; Hoell et al., 1990, 1993; Gregory et al., 1993a,b,c). These early instrument intercomparisons were conducted on a common aircraft platform and played an important role in understanding the sensitivity of different techniques and evaluating them to find the best possible field instrument. The early intercomparison effort stimulated the development of atmospheric measurement techniques/instruments benefitting airborne field programs to this day. Since early 2000, integrated field campaigns have made use of the same measurement technique on separate aircraft platforms or different measurement techniques sometimes on the same or separate aircraft platforms. To understand the differences seen in the data and to better utilize the data from various instruments, a careful and thorough intercomparison is needed. The first NASA two-aircraft intercomparison was conducted during the 2001 TRACE-P (Transport and Chemical Evolution over the Pacific) field campaign (Eisele et al., 2003). During TRACE-P the NASA DC-8 and P-3B flew wing-tip to wing-tip within 1 km of each other on three occasions lasting between 30 and 90 min. A significant finding of this exercise was that an intercomparison between two aircraft can reveal important insight into instrument performance. It also verified that two aircraft can be flown in a manner such that both sample the same air mass and experience the same high and low frequency fluctuations necessary to evaluate common measurements. In general the best agreement was achieved for the most abundant species (CO_2 and CH_4) with mixed results for less abundant species and those with shorter lifetimes (Eisele et al., 2003). The TRACE-P comparison of fast (1 s) measurements for CO and O_3 provided valuable information in defining bulk air mass properties, which was useful in interpreting the comparison results for short-lived species. The effect of small scale spatial variation should not have significant impact on assessment of the systematic difference, especially when the range of comparison is sufficiently larger than these variations.

Following TRACE-P, another major coordinated intercomparison occurred in 2004 during the International Consortium for Atmospheric Research on Transport and Transformation (ICARTT) airborne missions (INTEX-A, NEAQS-ITCT 2004, and ITOP). Five wing tip to wing tip intercomparison flights were conducted allowing comparisons between four aircraft. Although not formally published, these intercomparisons and additional mission information can be found in the Measurement Comparisons: ICARTT/INTEX-A link at <http://www-air.larc.nasa.gov/missions/intexna/intexna.htm>.

Table 1. Chemical Conditions for Intercomparison Periods.

Date	Air quality conditions	CO range (ppbv)
19 March 2006	Polluted urban and clean MBL off coast of Mexico	103–223
17 April 2006	Polluted and clean FT	99–163
15 May 2006	Clean FT and MBL off CA and OR coast	68–168

The purpose of this paper is to provide a straightforward and comprehensive overview and record of the measurement consistency as characterized through the analysis of the INTEX-B intercomparison data. This paper is not intended as a review of instrument operation but rather a means to highlight the demonstrated instrument performance during the intercomparison periods. Intercomparison results are intended to identify measurements where an investment in improving measurement capability would be of great benefit. Results are also crucial to ensuring that analysis and modeling activities based on multi-platform observations reach conclusions that can be supported within the assessed data uncertainties. For parties interested in making use of the data presented here, further consultation with the relevant measurement investigators is strongly recommended. The remainder of this paper presents the details of the INTEX-B intercomparison.

Section 3 describes the intercomparison approach and implementation, including a description of the types of comparisons is presented. Data processing procedures and statistical assessment are presented in Sect. 4. Section 5 contains the results, and the summary is contained in Sect. 6.

3 Approach/implementation

During the INTEX-B/MILAGRO/IMPEx field campaigns, three formal measurement comparisons were carried out on 19 March, 17 April, and 15 May 2006. These segments were well integrated into science flights to achieve the overall science goals while aiming to compare instruments/measurements under a wide variety of conditions as summarized in Table 1. During the intercomparison portion of the flights, aircraft separation was less than 300 m in the horizontal and less than 100 m in the vertical. The intercomparison period for the 19 March flight was 41 min (Fig. 1a), covered altitudes from 0.3 to 3.4 km, and encountered Mexico City pollution as well as marine boundary layer air off the coast of Mexico. The wide range of the chemical conditions is evident in CO levels observed during the intercomparison period which ranged from 103 to 223 ppbv. The 17 April (Fig. 1b) intercomparison period lasted 44 min with conditions ranging from polluted at 3.5 km over northern

California to clean at 6 km over southern Oregon. Again the range in chemical conditions can be inferred from the CO levels encountered (99 to 163 ppbv). The last intercomparison flight on 15 May (Fig. 1c) was the longest, lasting approximately 1 h. This intercomparison began in the clean free troposphere (about 5.5 km) off the northern Oregon coast and ended in the marine boundary layer (near 0.3 km) off the northern California coast. As with the two previous intercomparisons, a variety of chemical conditions existed. For these comparisons, data from all three flights were combined for analysis and only data with values greater than the limit of detection were used for analysis. The comparisons cover short-lived to long-lived gas phase species as well as particulate microphysical, optical, and chemical properties. Table 2 provides a detailed list of the species/parameters included in the intercomparison along with measurement techniques, aircraft platform, principal investigators (PI), measurement uncertainties, and confidence level. All of the above information was taken from the PI file headers except for confidence level. For an explanation of “Technique”, the reader is referred to the individual PI files located on the INTEX-B website (<http://www-air.larc.nasa.gov/missions/intex-b/intexb.html>) under the Current Archive Status link. The reported analysis was based on data submissions prior to 1 January 2010. The online plots may change to reflect the data updates at a later date.

In addition to the uncertainty information provided in the PI file headers, a special effort was made to obtain measurement uncertainties which were not originally provided in the file header as well as confidence levels. This is necessary information to determine if measurements are consistent and important metadata for future analysis. Some reported total uncertainties were given in 1 or 2 sigma confidence level while in other cases, confidence levels were not specified. The confidence level is typically associated with precision or precision dominated uncertainties. In some cases, both precision and accuracy are explicitly given in Table 2, while only total uncertainties are provided by the PI in many other cases without clear association to a confidence level. The concept of confidence level may be ill-defined for cases where accuracy is the dominant component of the total uncertainty. In these cases, the readers are directed to measurement PIs for proper application of the uncertainty information.

It is imperative that both aircraft sample the same air mass during the intercomparison period. In practice, this is conducted by keeping the aircraft in close proximity while maintaining a safe separation. Analysis of the fastest measurements can be an effective way to ensure the same air mass was sampled by both aircraft. If the same air mass is sampled, we expect the large scale features to be captured by both instruments. This is illustrated in the time series plots for both ozone (19 March) and water (15 May) where the major features are well represented by both instruments in each comparison (Figs. 2a and 3a). While the most prominent features are apparent in the data from each instrument, there is less

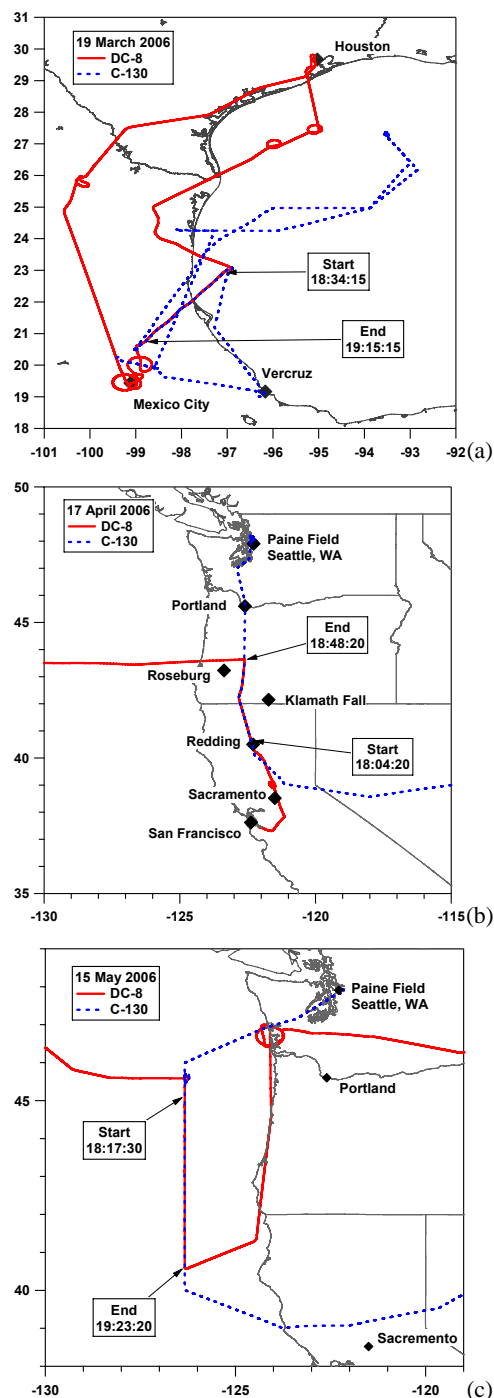


Fig. 1. (a) NASA DC-8 and NSF C-130 flights on 19 March 2006. The intercomparison period is indicated by the start and end times. The DC-8 flight path is shown as a solid red line. The C-130 flight path is shown as a blue dotted line. (b) NASA DC-8 and NSF C-130 flights on 17 April 2006. The intercomparison period is indicated by the start and end times. The DC-8 flight path is shown as a solid red line. The C-130 flight path is shown as a blue dotted line. (c) NASA DC-8 and NSF C-130 flights on 15 May 2006. The intercomparison period is indicated by the start and end times. The DC-8 flight path is shown as a solid red line. The C-130 flight path is shown as a blue dotted line.

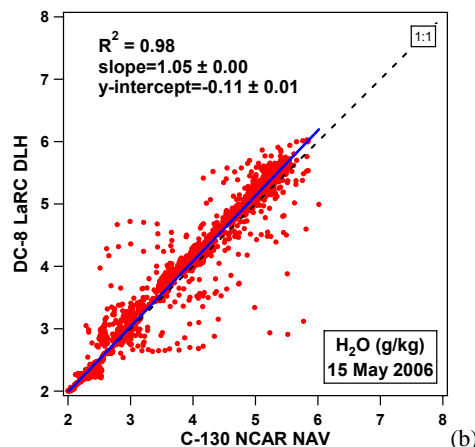
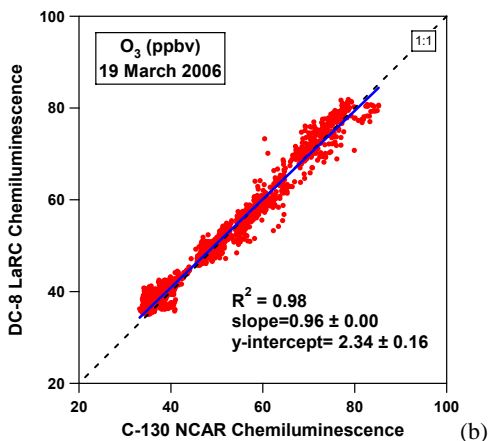
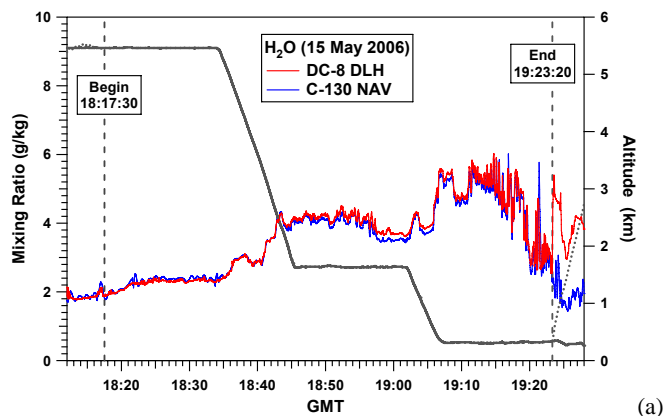
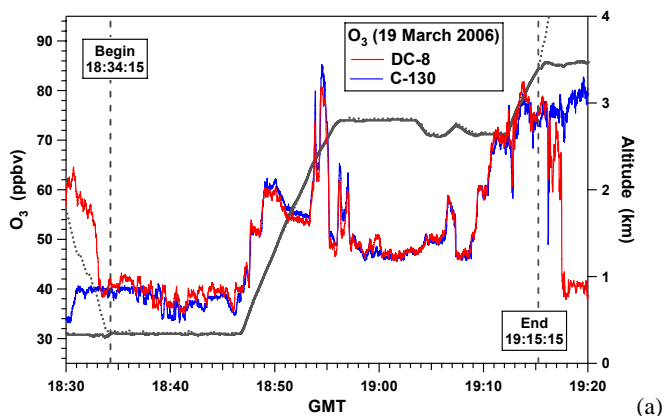


Fig. 2. (a) Timeseries for ozone during the intercomparison portion of the 19 March 2006 flight. The dotted line indicates the DC-8 altitude, solid thick line the C-130 altitude, red line DC-8 ozone, and blue line C-130 ozone. (b) Scatter plot and orthogonal distance regression for the DC-8 and C-130 ozone intercomparison on 19 March 2006.

Fig. 3. (a) Timeseries for water during the intercomparison portion of the 15 May 2006 flight. The dotted line indicates the DC-8 altitude, solid thick line the C-130 altitude, red line DC-8 ozone, and blue line C-130 ozone. (b) Scatter plot and orthogonal distance regression for the DC-8 and C-130 water intercomparison on 15 May 2006.

agreement in the relatively small scale changes that occur when O_3 remains consistently low (at low altitude in the marine boundary layer) and also at higher altitudes and higher O_3 levels (polluted Mexico City airmass). The timeseries for water displays a similar behavior. The large-scale features in the timeseries are well matched while there is less agreement in the finer features at both high (clean free troposphere) and low altitudes (marine boundary layer). The correlation plots (Figs. 2b and 3b) with associated regressions and coefficients of correlation (R^2) offer an additional method for evaluating the likelihood that the instruments sampled the same airmass. R^2 is defined as

$$R^2 = \frac{[\sum (x - \bar{x})(y - \bar{y})]^2}{\sum (x - \bar{x})^2 \sum (y - \bar{y})^2} \quad (1)$$

where \bar{x} is the average of the x values and \bar{y} is the average of the y values. Both ozone and water show that the measurements are strongly correlated as evident by the high R^2 value. Although it is not easy to discern in the time series for

water, there is a slight time lag in one of the water measurements. This is evident in Fig. 3b where data points depart the tighter cluster in curved lines. In general the spread in the data appears larger for water than ozone, however, this may be due in part to the smaller range in the x and y scales for water. The high R^2 value for both ozone and water nevertheless indicate that the two aircraft are most likely sampling the same airmass.

Intercomparison analysis was conducted during each stage of data submission: (1) comparison of field data (blind), (2) comparison of preliminary data (not blind), and (3) comparison of final data (not blind). These analyses and the distribution of results were carried out by the Measurement Comparison Working Group (MCWG). The primary responsibility of the MCWG included providing for secure field data submission to facilitate the “blind” comparison, analyzing data for each stage of data submission, and disseminating the results within the science team and to the

Table 2. Summary of Intercomparison Measurements.

Species	Technique ^a	Aircraft	Principal Investigator	Uncertainty ^b	Confidence Level
CO	UVF DACOM	C-130 DC-8	T. Campos, NCAR G. Sachse, NASA LaRC	10% 2% or 2 ppbv (1 sigma $p = 1%$ or 1 ppbv, $a = 2%$)	Contact PI Contact PI
H ₂ O	Cryo Cryo DLH	DC-8 C-130 DC-8	J. Barrick, NASA LaRC, UND/NSERC Allen Schanot, NCAR/RAF G. Diskin, NASA LaRC	5% ± 0.5 C; ± 1 C below a dp of -60 C 5% (1 sigma $p = 1%$ or 0.05 ppmv, $a = 5%$ or 1 ppmv)	2 sigma Contact PI Contact PI
NO	CLD CLD	C-130 DC-8	A. Weinheimer, NCAR G. Huey, GIT	10 pptv or 10% (6.83, 85.71) 25% ^c	1 sigma 2 sigma
NO ₂	CLD TD-LIF	C-130 DC-8	A. Weinheimer, NCAR R. Cohen, UC Berkeley	20 pptv or 15% 15 pptv + (0.05 \times value) ^d ($a = 5%$)	1 sigma 2 sigma
O ₃	CLD CLD	DC-8 C-130	M. Avery, NASA LaRC A. Weinheimer, NCAR	3 ppb or 3% dry air, 5–7% moist air ($p < 1$ ppbv, 2 sigma) 0.1 ppbv or 5%	Contact PI 1 sigma
SO ₂	CIMS UVF CIMS	DC-8 C-130 C-130	G. Huey, GIT J. Holloway, NOAA P. Wennberg, CIT	15% 15% + 0.8 ppbv ($p = 0.8$ ppbv, 2 sigma) 35% + 0.2 ppbv + 0.2 \times formic acid	2 sigma 2 sigma Contact PI
HCN	CIMS PANAK	C-130 DC-8	P. Wennberg, CIT H. Singh, NASA ARC	$\pm 20\% + 50$ pptv $\pm 15\%$	Contact PI 1 sigma
CH ₃ CN	TOGA PANAK PTRMS	C-130 DC-8 C-130	E. Apel, NCAR H. Singh, NASA ARC T. Karl, NCAR/ACD	20% $\pm 15\%$ 35% ($a = 15\%$)	1 sigma 1 sigma 1 sigma
Propanal	TOGA PANAK	C-130 DC-8	E. Apel, NCAR H. Singh, NASA ARC	20% 50%	1 sigma 1 sigma
CH ₂ O	DFG TDL EFD	C-130 DC-8 DC-8	P. Weibring, NCAR A. Fried, NCAR B. Heikes, URI	(13.45, 97.67) 17.16% ^c (15.15, 269.8) 37.3% ^c (17.61, 81.48) 19.3% ^c	2 sigma 2 sigma Contact PI
CH ₃ OOH	CIMS EFD	C-130 DC-8	P. Wennberg, CIT B. Heikes, URI	50% + 250 pptv 135 + (0.25 \times value)	Contact PI Contact PI
H ₂ O ₂	CIMS EFD ACCD	C-130 DC-8 DC-8	P. Wennberg, CIT B. Heikes, URI D. O'Sullivan, USNA	25% + 100 pptv 15 + (0.15 \times value) 30 pptv + 0.35 \times value	Contact PI Contact PI 2 sigma
HNO ₃	CIMS TD-LIF MC	C-130 DC-8 DC-8	P. Wennberg, CIT R. Cohen, UC Berkeley R. Talbot, UNH	30% + 50 pptv (23.43, 97.85) 43.7% ^c <25 pptv = 30–35%; 25–100 pptv = 20%; >100 pptv = 15%	Contact PI 2 sigma 1 sigma
PAN	CIGAR PANAK	C-130 DC-8	F. Flocke, NCAR/ACD H. Singh, NASA ARC	($p = 9%$, $a = 10\% + 18$ pptv) 10% (>100 pptv); 15% (<100 pptv)	2 sigma 1 sigma
Total PANs ^e	CIGAR TD-LIF	C-130 DC-8	F. Flocke, NCAR/ACD R. Cohen, UC Berkeley	($p = 9%$, $a = 10\% + 18$ pptv) 20 pptv + (0.1 \times value) ^d	2 sigma 2 sigma
NO _y -NO	CLD TD-LIF	C-130 DC-8	A. Weinheimer, NCAR R. Cohen, UC Berkeley	Derived quantity from NO _y and NO (13, 78) 35% ^c	Contact PI 2 sigma
OH	CIMS ATHOS	C-130 DC-8	L. Mauldin, NCAR W. Brune, Penn State	35% ($a = 32%$, 2 sigma)	2 sigma Contact PI
HO ₂	CIMS ATHOS	C-130 DC-8	C. Cantrell, NCAR W. Brune, Penn State	35% ($a = 32%$, 2 sigma)	2 sigma Contact PI
Acetaldehyde	TOGA PANAK PTRMS	C-130 DC-8 C-130	E. Apel, NCAR H. Singh, NASA ARC T. Karl, NCAR/ACD	20% 50% 35%	1 sigma 1 sigma 1 sigma
Acetone	TOGA PANAK	C-130 DC-8	E. Apel, NCAR H. Singh, NASA ARC	20% 20%	1 sigma 1 sigma
Ethanol	TOGA PANAK	C-130 DC-8	E. Apel, NCAR H. Singh, NASA ARC	20% 20%	1 sigma 1 sigma
MEK	TOGA PANAK PTRMS	C-130 DC-8 C-130	E. Apel, NCAR H. Singh, NASA ARC T. Karl, NCAR/ACD	20% 20% 35%	1 sigma 1 sigma 1 sigma
Methanol	TOGA PANAK PTRMS	C-130 DC-8 C-130	E. Apel, NCAR H. Singh, NASA ARC T. Karl, NCAR/ACD	20% 20% 35%	1 sigma 1 sigma 1 sigma
All NMHCs	WAS	DC-8/C-130	D. Blake, UCI	5%	1 sigma
$j(\text{O}_3)$	SAFS	DC-8/C-130	R. Shetter, ARIM/NCAR	See footnote e	Contact PI
$j(\text{NO}_2)$	SAFS Filt. Rad	DC-8/C-130 DC-8	R. Shetter, ARIM/NCAR J. Barrick, NASA LaRC	See footnote e 8%	Contact PI 2 sigma

Table 2. Continued.

Species	Technique ^a	Aircraft	Principal Investigator	Uncertainty ^b	Confidence Level
$N > 3$ nm	CPC	DC-8	B. Anderson, LaRC/A. Clarke, U Hawaii	10%	Contact PI
	CPC	C-130	A. Clarke, U Hawaii	10%	Contact PI
$N > 10$ nm (05/15)	CPC	DC-8	B. Anderson, LaRC/A. Clarke, U Hawaii	5%	Contact PI
	CPC	C-130	A. Clarke, U Hawaii	5%	Contact PI
$N > 10$ nm (04/17)	CPC	DC-8	B. Anderson, LaRC/A. Clarke, U Hawaii	5%	Contact PI
	CPC	C-130	A. Clarke, U Hawaii	5%	Contact PI
Hot CN (03/19)	CPC	DC-8	B. Anderson, LaRC/A. Clarke, U Hawaii	5%	Contact PI
	CPC	C-130	A. Clarke, U Hawaii	5%	Contact PI
Hot CN (05/15)	CPC	DC-8	B. Anderson, LaRC/A. Clarke, U Hawaii	5%	Contact PI
	CPC	C-130	A. Clarke, U Hawaii	5%	Contact PI
N_DMA	DMA	DC-8	B. Anderson, LaRC/A. Clarke, U Hawaii	15%	Contact PI
	DMA	C-130	A. Clarke, U Hawaii	15%	Contact PI
N_OPC	OPC	DC-8	B. Anderson, LaRC/A. Clarke, U Hawaii	15%	Contact PI
	OPC	C-130	A. Clarke, U Hawaii	15%	Contact PI
N_APS	APS	DC-8	B. Anderson, LaRC/A. Clarke, U Hawaii	15%	Contact PI
	APS	C-130	A. Clarke, U Hawaii	15%	Contact PI
Nsub	OPC	DC-8	B. Anderson, LaRC/A. Clarke, U Hawaii	15%	Contact PI
	OPC	C-130	A. Clarke, U Hawaii	15%	Contact PI
Nsuper	OPC	DC-8	B. Anderson, LaRC/A. Clarke, U Hawaii	15%	Contact PI
	OPC	C-130	A. Clarke, U Hawaii	15%	Contact PI
N_150C_DMA	DMA	DC-8	B. Anderson, LaRC/A. Clarke, U Hawaii	15%	Contact PI
	DMA	C-130	A. Clarke, U Hawaii	15%	Contact PI
N_150C_OPC	OPC	DC-8	B. Anderson, LaRC/A. Clarke, U Hawaii	15%	Contact PI
	OPC	C-130	A. Clarke, U Hawaii	15%	Contact PI
Nsub_150C	OPC	DC-8	B. Anderson, LaRC/A. Clarke, U Hawaii	15%	Contact PI
	OPC	C-130	A. Clarke, U Hawaii	15%	Contact PI
Nsuper_150C	OPC	DC-8	B. Anderson, LaRC/A. Clarke, U Hawaii	15%	Contact PI
	OPC	C-130	A. Clarke, U Hawaii	15%	Contact PI
N_300C_DMA	DMA	DC-8	B. Anderson, LaRC/A. Clarke, U Hawaii	15%	Contact PI
	DMA	C-130	A. Clarke, U Hawaii	15%	Contact PI
N_300C_OPC	OPC	DC-8	B. Anderson, LaRC/A. Clarke, U Hawaii	15%	Contact PI
	OPC	C-130	A. Clarke, U Hawaii	15%	Contact PI
Nsub_300C	OPC	DC-8	B. Anderson, LaRC/A. Clarke, U Hawaii	15%	Contact PI
	OPC	C-130	A. Clarke, U Hawaii	15%	Contact PI
Nsuper_300C	OPC	DC-8	B. Anderson, LaRC/A. Clarke, U Hawaii	15%	Contact PI
	OPC	C-130	A. Clarke, U Hawaii	15%	Contact PI
N_400C_OPC	OPC	DC-8	B. Anderson, LaRC/A. Clarke, U Hawaii	15%	Contact PI
	OPC	C-130	A. Clarke, U Hawaii	15%	Contact PI
Nsub_400C	OPC	DC-8	B. Anderson, LaRC/A. Clarke, U Hawaii	15%	Contact PI
	OPC	C-130	A. Clarke, U Hawaii	15%	Contact PI
Nsuper_400C	OPC	DC-8	B. Anderson, LaRC/A. Clarke, U Hawaii	15%	Contact PI
	OPC	C-130	A. Clarke, U Hawaii	15%	Contact PI
V_DMA	DMA	DC-8	B. Anderson, LaRC/A. Clarke, U Hawaii	30%	Contact PI
	DMA	C-130	A. Clarke, U Hawaii	30%	Contact PI
V_OPC	OPC	DC-8	B. Anderson, LaRC/A. Clarke, U Hawaii	30%	Contact PI
	OPC	C-130	A. Clarke, U Hawaii	30%	Contact PI
V_APS	APS	DC-8	B. Anderson, LaRC/A. Clarke, U Hawaii	30%	Contact PI
	APS	C-130	A. Clarke, U Hawaii	30%	Contact PI
Vsub	OPC	DC-8	B. Anderson, LaRC/A. Clarke, U Hawaii	30%	Contact PI
	OPC	C-130	A. Clarke, U Hawaii	30%	Contact PI
Vsuper	OPC	DC-8	B. Anderson, LaRC/A. Clarke, U Hawaii	30%	Contact PI
	OPC	C-130	A. Clarke, U Hawaii	30%	Contact PI
V_150C_DMA	DMA	DC-8	B. Anderson, LaRC/A. Clarke, U Hawaii	30%	Contact PI
	DMA	C-130	A. Clarke, U Hawaii	30%	Contact PI
V_150C_OPC	OPC	DC-8	B. Anderson, LaRC/A. Clarke, U Hawaii	30%	Contact PI
	OPC	C-130	A. Clarke, U Hawaii	30%	Contact PI
Vsub_150C	OPC	DC-8	B. Anderson, LaRC/A. Clarke, U Hawaii	30%	Contact PI
	OPC	C-130	A. Clarke, U Hawaii	30%	Contact PI

Table 2. Continued.

Species	Technique ^a	Aircraft	Principal Investigator	Uncertainty ^b	Confidence Level
Vsuper_150C	OPC	DC-8	B. Anderson, LaRC/A. Clarke, U Hawaii	30%	Contact PI
	OPC	C-130	A. Clarke, U Hawaii	30%	Contact PI
V_300C_DMA	DMA	DC-8	B. Anderson, LaRC/A. Clarke, U Hawaii	30%	Contact PI
	DMA	C-130	A. Clarke, U Hawaii	30%	Contact PI
V_300C_OPC	OPC	DC-8	B. Anderson, LaRC/A. Clarke, U Hawaii	30%	Contact PI
	OPC	C-130	A. Clarke, U Hawaii	30%	Contact PI
Vsub_300C	OPC	DC-8	B. Anderson, LaRC/A. Clarke, U Hawaii	30%	Contact PI
	OPC	C-130	A. Clarke, U Hawaii	30%	Contact PI
Vsuper_300C	OPC	DC-8	B. Anderson, LaRC/A. Clarke, U Hawaii	30%	Contact PI
	OPC	C-130	A. Clarke, U Hawaii	30%	Contact PI
V_400C_OPC	OPC	DC-8	B. Anderson, LaRC/A. Clarke, U Hawaii	30%	Contact PI
	OPC	C-130	A. Clarke, U Hawaii	30%	Contact PI
Vsub_400C	OPC	DC-8	B. Anderson, LaRC/A. Clarke, U Hawaii	30%	Contact PI
	OPC	C-130	A. Clarke, U Hawaii	30%	Contact PI
Vsuper_400C	OPC	DC-8	B. Anderson, LaRC/A. Clarke, U Hawaii	30%	Contact PI
	OPC	C-130	A. Clarke, U Hawaii	30%	Contact PI
SO ₄ ⁻	MC	DC-8	J. Dibb, UNH	10% + 5 pptv	1 sigma
	AMS	C-130	J. Jimenez, U CO	0.04 µg s m ⁻³ (<i>a</i> = 35%, 2 sigma) ^g	2 sigma
	PILS	C-130	R. Weber, GIT	Conc > 2 × LOD = 20% Conc < = 2 × LOD = 40%	1 sigma
NO ₃ ⁻	AMS	C-130	J. Jimenez, U CO	0.06 µg s m ⁻³ (<i>a</i> = 35%, 2 sigma) ^g	2 sigma
	PILS	C-130	R. Weber, GIT	Conc > 2 × LOD = 20% Conc < = 2 × LOD = 40%	1 sigma
NH ₄ ⁺	AMS	C-130	J. Jimenez, U CO	0.36 µg s m ⁻³ (<i>a</i> = 35%, 2 sigma) ^g	2 sigma
	PILS	C-130	R. Weber, GIT	Conc > 2 × LOD = 20% Conc < = 2 × LOD = 40%	1 sigma
Scatt 450 nm	TSI Nephelometer	DC-8	B. Anderson, LaRC/A. Clarke, U Hawaii	10% or 0.5 Mm ⁻¹	Contact PI
	TSI Nephelometer	C-130	A. Clarke, U Hawaii	10% or 0.5 Mm ⁻¹	Contact PI
Scatt 550 nm	TSI Nephelometer	DC-8	B. Anderson, LaRC/A. Clarke, U Hawaii	10% or 0.5 Mm ⁻¹	Contact PI
	TSI Nephelometer	C-130	A. Clarke, U Hawaii	10% or 0.5 Mm ⁻¹	Contact PI
Scatt 700 nm	TSI Nephelometer	DC-8	B. Anderson, LaRC/A. Clarke, U Hawaii	10% or 0.5 Mm ⁻¹	Contact PI
	TSI Nephelometer	C-130	A. Clarke, U Hawaii	10% or 0.5 Mm ⁻¹	Contact PI
Scattsub 550 nm	RR Nephelometer	DC-8	B. Anderson, LaRC/A. Clarke, U Hawaii	10% or 0.5 Mm ⁻¹	Contact PI
	RR Nephelometer	C-130	A. Clarke, U Hawaii	10% or 0.5 Mm ⁻¹	Contact PI
Abs 470 nm	PSAP	DC-8	B. Anderson, LaRC/A. Clarke, U Hawaii	20% or 0.5 Mm ⁻¹	Contact PI
	PSAP	C-130	A. Clarke, U Hawaii	20% or 0.5 Mm ⁻¹	Contact PI
Abs 530 nm	PSAP	DC-8	B. Anderson, LaRC/A. Clarke, U Hawaii	20% or 0.5 Mm ⁻¹	Contact PI
	PSAP	C-130	A. Clarke, U Hawaii	20% or 0.5 Mm ⁻¹	Contact PI
Abs 660 nm	PSAP	DC-8	B. Anderson, LaRC/A. Clarke, U Hawaii	20% or 0.5 Mm ⁻¹	Contact PI
	PSAP	C-130	A. Clarke, U Hawaii	20% or 0.5 Mm ⁻¹	Contact PI

^a For an explanation of “Technique”, the reader is referred to the individual PI files located on the INTEX-B website (<http://www-air.larc.nasa.gov/missions/intex-b/intexb.html>) under the Current Archive Status link.

^b Total uncertainty unless otherwise specified. Precision (*p*) and accuracy (*a*) given in parentheses.

^c Absolute uncertainty reported point-by-point. Percent uncertainty for the intercomparison period is calculated, minimum and maximum given in parentheses, median given outside the parentheses.

^d Uncertainty for one second data reported point-by-point in file header. For consistency, values shown are PI estimates for 60 s averages.

^e No PI reported uncertainty.

^f PANs = Peroxy alkyl nitrates, formula R-C(O)OONO₂, with R = liphatic, olefinic, or substituted aliphatic or olefinic substituent.

^g Uncertainty given for 12 second integration time. For further details, PI refers the reader to Dunlea et al. (2009) and Bahreini et al. (2009).

atmospheric community at large. In stage one, the blind comparison of field data, PIs submitted data within 24 h to a few days after the flight to an ftp site which was “blind” to the science team for a period of time until both paired comparison data were submitted. For example, the CO data was not available to the science team until both NSF C-130 and NASA DC-8 PIs submitted their CO data for

the intercomparison flight. The MCWG then assessed the consistency between the paired DC-8 and C-130 measurements/instruments and released the comparison results and the data to the science team. In the preliminary data stage, data were compared again after allowing the PIs to apply post mission calibration and additional processing/correction procedures to their data. The MCWG presented these

Table 3a. Statistical results of DC-8/C-130 intercomparison. Photochemical precursors and gas phase tracers. NOTE: Technique is listed as X (C-130) vs. Y (DC-8).

Species	Technique	Units	Slope	Intercept	R^2	Ratio Percentiles			# Pts	Range	
						25th	50th	75th		Min	Max
CO	UVF vs. DACOM	ppbv	1.09 ± 0.00	-5.1 ± 0.2	0.99				7823	68.5	223
H ₂ O	Cryo vs. DLH	g kg^{-1}	0.92 ± 0.00	0.15 ± 0.0	0.99				8928	> .0006	16.5
	Cryo vs. Cryo	g kg^{-1}	0.94 ± 0.00	0.05 ± 0.0	0.99				9050	0.02	16.5
NO	CLD vs. CLD	pptv	0.95 ± 0.01	13.1 ± 0.2	0.81				5277	LOD	205
NO ₂	CLD vs. TD-LIF	pptv	1.20 ± 0.01	-39 ± 1	0.87				2254	LOD	796
O ₃	CLD vs. CLD	ppbv	1.00 ± 0.00	-1.0 ± 0.1	0.99				6408	26.2	133
SO ₂	CIMS vs. CIMS	pptv	0.56 ± 0.00	3 ± 16	0.98				307	3	21 610
	UVF vs. CIMS	pptv	0.86 ± 0.01	-486 ± 27	0.97				434	230	14 700
HCN	CIMS vs. PANAK	pptv			0.37	0.50	0.69	0.90	22	150	2272
CH ₃ CN ^a	TOGA vs. PANAK	pptv			0.06	0.78	1.02	1.15	16	0.03	0.29
	PTRMS vs. PANAK	pptv			0.61	0.64	0.83	0.95	16	0.04	0.29
Propanal ^a	TOGA vs. PANAK	pptv			0.38	0.63	1.23	1.86	10	0.005	0.18

^a Online files found in VOCs link at <http://www-air.larc.nasa.gov/missions/intex-b/intexb.html> under the Measurement Comparisons: MILAGRO/INTEX-B/IMPEX link.

Table 3b. Statistical results of DC-8/C-130 intercomparison. Photochemical products. NOTE: Technique is listed as X (C-130) vs. Y (DC-8).

Species	Technique	Units	Slope	Intercept	R^2	Ratio Percentiles			# Pts	Range	
						25th	50th	75th		Min	Max
CH ₂ O	DFG vs. EFD	pptv	1.12 ± 0.09	-401 ± 152	0.88				24	LOD	3687
	DFG vs. TDL	pptv	1.01 ± 0.03	19 ± 33	0.95				67	LOD	3861
CH ₃ OOH	CIMS vs. EFD	pptv			0.30	0.87	1.13	1.41	26	217	2286
H ₂ O ₂	CIMS vs. EFD	pptv	1.24 ± 0.04	-19 ± 67	0.92				74	41	2809
	CIMS vs. ACCD	pptv	0.84 ± 0.02	313 ± 21	0.83				392	80	2314
HNO ₃	CIMS vs. MC	pptv	1.21 ± 0.04	-3 ± 14	0.88				98	10	1302
	CIMS vs. TDLIF	pptv			0.63	0.57	0.66	0.80	45	78	1749
PAN	CIGAR vs. PANAK	pptv	1.68 ± 0.16	-185 ± 59	0.77				33	2	1986
Total PAN	CIGAR vs. TDLIF	pptv	1.35 ± 0.03	-83 ± 10	0.94				157	LOD	2175
NO _y -NO	CLD vs. TD-LIF	pptv	0.92 ± 0.01	51 ± 18	0.97				143	133	5559

results to the science team at the post-mission data workshop. In the comparison of final data (not blind), PIs submitted final data with uncertainty estimates. These results are archived online (<http://www-air.larc.nasa.gov/missions/intex-b/intexb-meas-comparison.htm>) and summarized here.

In addition to the inter-platform comparisons, intra-platform comparisons were made whenever possible. Since both instruments were located on the same aircraft, these comparisons were not limited to the three intercomparison periods discussed previously, rather they could span the entire mission.

As previously stated, the primary goal of this paper is to present a comprehensive overview of the INTEX-B/MILAGRO/IMPEX intercomparison results and provide a record of the measurement consistency. The level of the agreement between the measurements may depend on a number of factors, including calibration, instrument time re-

sponse, and measurement techniques. For the comparison of the aerosol measurements, the particle size range of the measurements should be a critical consideration. The information summarized in Table 2 and Tables 3–5 is critical to determine if observations made from different platforms/instruments are consistent within the PI reported uncertainties. This is necessary when deciding if multiple data sets should be used in integrated analysis. At the same time, users are cautioned that differences between measurements can still be significant, even though they are technically consistent within the combined uncertainties quoted by the PIs. In addition, this overview paper does not attempt to describe the complexities of the various measurement techniques. Any interpretation of the results of these studies should be done in consultation with the individual instrument PIs (provided in Table 2).

Table 3c. Statistical results of DC-8/C-130 intercomparison. Photochemical radicals. NOTE: Technique is listed as X (C-130) vs. Y (DC-8).

Species	Technique	Units	Slope	Intercept	R^2	Ratio Percentiles			# Pts	Range	
						25th	50th	75th		Min	Max
OH	CIMS vs. ATHOS	pptv			0.03	0.41	0.81	1.06	266	0.003	0.62
HO ₂	CIMS vs. ATHOS	pptv			0.59	0.98	1.23	1.73	107	LOD	64.4

Table 3d. Statistical results of DC-8/C-130 intercomparison. Oxygenated volatile organic carbons. NOTE: Technique is listed as X (C-130) vs. Y (DC-8).

Species	Technique	Units	Slope	Intercept	R^2	Ratio Percentiles			# Pts	Range	
						25th	50th	75th		Min	Max
Acetaldehyde ^a	TOGA vs. PANAK	pptv	1.27 ± 0.10	0.02 ± 0.04	0.93				14	0.02	1.3
	PTRMS vs. PANAK	pptv	1.31 ± 0.21	0.03 ± 0.10	0.78				12	0.04	1.3
Acetone	TOGA vs. PANAK	pptv			0.50	1.05	1.42	1.82	16	0.24	3.0
Ethanol ^a	TOGA vs. PANAK	pptv							4		
MEK ^a	TOGA vs. PANAK	pptv	0.62 ± 0.07	0.00 ± 0.01	0.84				16	0.01	0.22
Methanol ^a	TOGA vs. PANAK	pptv			0.47	1.31	2.51	3.36	16	0.20	6.6
	PTRMS vs. PANAK	pptv			0.25	1.60	2.09	2.57	16	0.25	11.5

^a Online files found in VOCs link at <http://www-air.larc.nasa.gov/missions/intex-b/intexb.html> under the Measurement Comparisons: MILAGRO/INTEX-B/IMPEX link.

4 Data process procedures and statistical assessment

The quantitative assessment of measurement/instrument consistency was based on statistical analysis of the intercomparison data. This required the merging of data to a common timeline. Merging was easiest when measurements were conducted with the same timing and integration period; however, it is not unusual for instruments based on different techniques to require different integration times to measure the same species/parameter or that instruments on different platforms are not well synchronized. For cases where instruments had the same integration period, but were not synchronized, the data were merged to ensure at least 50% sampling time overlap. For paired measurements with different integration time intervals, the shorter integration time measurements were merged into the longer time interval when measurements at the shorter time interval overlapped at least 50% of the longer time interval. These merged data pairs were used to quantitatively assess measurement consistency through linear regression analysis, when applicable, or descriptive statistics based on the ratio (DC-8/C-130) of the paired data points. The linear regression slopes and intercepts can be used to describe the level of the measurement agreement when a high enough level of correlation exists. Here, this criteria has been defined as an R^2 value of 0.75. Lower R^2 values are typically encountered when the range of variation is limited in comparison to the uncertainties of the measurements and/or other instrument issues exist. When R^2 is below the threshold of 0.75, the median and percentile values of the DC-8/C-130 ratio have been used to express the

level of consistency between the paired data. In addition, the absolute (or arithmetic) difference between paired data may be used in some cases (with combined uncertainties) to gain additional insight.

Statistical comparisons presented here have been based on Orthogonal Distance Regression (ODR). Orthogonal distance regression is a regression technique similar to ordinary least squares (OLS) fit with the stipulation that both x and y are independent variables with errors. ODR minimizes sum of the squares of the orthogonal distances rather than the vertical distances (as in OLS). ODR is generally equivalent to

$$\min_{\beta, \delta, \varepsilon} \frac{1}{2} \sum_{i=1}^n \left(w_{\varepsilon_i} \varepsilon_i^2 + w_{\delta_i} \delta_i^2 \right) \quad (2)$$

subject to $y_i + \varepsilon_i = f(x_i + \delta_i; \beta)$ where ε_i is the error in y , δ_i the error in x , w_{ε_i} and w_{δ_i} weighting factors, and β a vector of parameters to be determined (slope and intercept in this case), (Zwolak et al., 2007). Note that a weighted ODR (w_{ε_i} and $w_{\delta_i} \neq 1$) is necessary when observations x_i and y_i are heteroscedastic (variance changes with i), (Boggs et al., 1988). It has been shown that ODR performs at least as well and in many cases significantly better than Ordinary Least Squares (OLS), especially when $d\sigma_{\varepsilon}/\sigma_{\delta} < 2$, (Boggs et al., 1988). Boggs et al. (1988) have shown that ODR results in smaller bias, variance, and mean square error (mse) than OLS, except possibly when significant outliers are present in the data. For the bias of the parameter, β , and function estimates, $f(x_i; \beta)$, OLS is statistically better only 2% of the time while ODR is significantly better 50% of the time. Results for the variance and mse of the parameter and function

Table 3e. Statistical results of DC-8/C-130 intercomparison. Nonmethane hydrocarbons, halocarbons, alkylnitrates, and organic sulfur compounds. NOTE: Technique is listed as X (C-130) vs. Y (DC-8).

Species	Technique	Units	Slope	Intercept	R^2	Ratio Percentiles			# Pts	Range	
						25th	50th	75th		Min	Max
DMS ^a	WAS vs. WAS	pptv							3	2	8
OCS ^a	WAS vs. WAS	pptv			0.41	0.98	1.00	1.01	39	451	504
CS ₂ ^a	WAS vs. WAS	pptv			0.30	0.96	1.58	2.53	38	3	30
CFC-11 ^b	WAS vs. WAS	pptv			0.13	1.00	1.00	1.01	40	246	256
CFC-12 ^b	WAS vs. WAS	pptv			0.28	1.00	1.00	1.00	40	525	538
CFC-113 ^b	WAS vs. WAS	pptv			0.09	1.00	1.00	1.01	40	77	79
CFC-114 ^b	WAS vs. WAS	pptv			0.06	0.99	1.00	1.01	40	15	15
H-1211 ^b	WAS vs. WAS	pptv			0.25	1.01	1.02	1.03	40	4	4
H-1301 ^b	WAS vs. WAS	pptv			0.00	0.96	0.99	1.00	40	3	3
H-2402 ^b	WAS vs. WAS	pptv			0.19	1.00	1.00	1.02	40	0.48	0.51
HCFC-22 ^b	WAS vs. WAS	pptv	0.86 ± 0.05	23 ± 8	0.80				40	162	180
HCFC-141b ^b	WAS vs. WAS	pptv	0.88 ± 0.04	2.35 ± 0.77	0.84				40	17	20
HCFC-142b ^b	WAS vs. WAS	pptv			0.51	0.98	1.00	1.02	40	15	17
HFC-134a ^b	WAS vs. WAS	pptv	0.99 ± 0.06	0.81 ± 2.20	0.75				40	33	41
CHCl ₃ ^b	WAS vs. WAS	pptv	1.00 ± 0.03	0.4 ± 0.3	0.93				40	15	17
CH ₂ Cl ₂ ^b	WAS vs. WAS	pptv	0.98 ± 0.54	0.96 ± 0.02	0.97				40	20	42
CCl ₄ ^b	WAS vs. WAS	pptv			0.13	1.00	1.01	1.01	40	91	95
C ₂ Cl ₄ ^b	WAS vs. WAS	pptv	0.99 ± 0.03	0.05 ± 0.12	0.94				40	1	7
C ₂ HCl ₃ ^b	WAS vs. WAS	pptv			0.48	1.72	3.89	5.59	40	0.02	1
CH ₃ Cl ^b	WAS vs. WAS	pptv	0.96 ± 0.02	21 ± 10	0.98				40	508	873
Ethylchloride ^b	WAS vs. WAS	pptv			0.63	0.84	0.96	1.05	40	2	6
CH ₃ Br ^b	WAS vs. WAS	pptv	0.74 ± 0.05	2.4 ± 0.4	0.75				40	7	10
CH ₃ I ^b	WAS vs. WAS	pptv	1.11 ± 0.04	0.02 ± 0.02	0.91				40	0.03	1
CH ₂ Br ₂ ^b	WAS vs. WAS	pptv	0.91 ± 0.04	0.12 ± 0.04	0.88				40	0.73	2
CHBrCl ₂ ^b	WAS vs. WAS	pptv	0.90 ± 0.04	0.02 ± 0.01	0.89				40	0.12	0.28
CHBr ₂ Cl ^b	WAS vs. WAS	pptv	0.91 ± 0.04	0.02 ± 0.01	0.85				40	0.07	0.35
CHBr ₃ ^b	WAS vs. WAS	pptv	0.92 ± 0.03	0.07 ± 0.03	0.92				40	0.21	3
1,2-Dichloroethane ^b	WAS vs. WAS	pptv	0.96 ± 0.03	0.16 ± 0.31	0.92				40	5	16
MeONO ₂ ^c	WAS vs. WAS	pptv	1.00 ± 0.00	-0.02 ± 0.11	0.94				40	2	5
EtONO ₂ ^c	WAS vs. WAS	pptv	0.93 ± 0.03	0.10 ± 0.05	0.95				40	0.73	3
i-PrONO ₂ ^c	WAS vs. WAS	pptv	0.96 ± 0.04	0.06 ± 0.20	0.88				40	0.58	9
n-PrONO ₂ ^c	WAS vs. WAS	pptv	0.94 ± 0.04	0.02 ± 0.03	0.86				40	0.07	1
2-BuONO ₂ ^c	WAS vs. WAS	pptv	0.86 ± 0.03	0.01 ± 0.18	0.85				40	0.21	11
2-PenONO ₂ ^c	WAS vs. WAS	pptv	1.29 ± 0.08	-0.38 ± 0.12	0.86				24	0.08	3
3-PenONO ₂ ^c	WAS vs. WAS	pptv	0.93 ± 0.07	-0.03 ± 0.07	0.77				25	0.06	2
3-Methyl-2-BuONO ₂ ^c	WAS vs. WAS	pptv	1.22 ± 0.06	-0.31 ± 0.09	0.89				24	0.04	3
Ethane ^a	WAS vs. WAS	pptv	1.00 ± 0.01	-1.2 ± 7.9	0.99				40	386	1664
Ethene ^a	WAS vs. WAS	pptv	1.00 ± 0.04	-1.0 ± 5.6	0.96				13	12	299
Ethyne ^a	WAS vs. WAS	pptv	1.00 ± 0.01	0.06 ± 2.7	0.99				40	32	570
Propane ^a	WAS vs. WAS	pptv	0.85 ± 0.07	-107 ± 32	0.75				40	10	792
Propene ^a	WAS vs. WAS	pptv							5	4	12
i-Butane ^a	WAS vs. WAS	pptv	0.95 ± 0.03	1.8 ± 1.4	0.96				24	11	154
n-Butane ^a	WAS vs. WAS	pptv	0.94 ± 0.02	3.8 ± 1.9	0.97				24	22	416
1-Butene ^a	WAS vs. WAS	pptv							0		
Trans-2-Butene ^a	WAS vs. WAS	pptv							0		
Cis-2-Butene ^a	WAS vs. WAS	pptv							0		
1,3-Butadiene ^a	WAS vs. WAS	pptv							0		
Isoprene ^a	WAS vs. WAS	pptv							1		
i-Pentane ^a	WAS vs. WAS	pptv	0.99 ± 0.03	1.7 ± 1.3	0.97				24	5	181
n-Pentane ^a	WAS vs. WAS	pptv	0.96 ± 0.03	0.18 ± 0.72	0.96				23	5	74
2-Methylpentane ^a	WAS vs. WAS	pptv							8		
3-Methylpentane ^a	WAS vs. WAS	pptv							4	4	31
n-Hexane ^a	WAS vs. WAS	pptv	1.1 ± 0.08	-1.9 ± 0.66	0.97				16	4	36

Table 3e. Continued.

Species	Technique	Units	Slope	Intercept	R^2	Ratio Percentiles			# Pts	Range	
						25th	50th	75th		Min	Max
n-Heptane ^a	WAS vs. WAS	pptv							1		
Benzene ^a	WAS vs. WAS	pptv	0.98 ± 0.01	-0.29 ± 0.78	0.99				36	4	138
1,2,4-Trimethylbenzene ^a	WAS vs. WAS	pptv							0		
1,3,5-Trimethylbenzene ^a	WAS vs. WAS	pptv							0		
Ethylbenzene ^a	WAS vs. WAS	pptv							3	4	17
i-Propylbenzene ^a	WAS vs. WAS	pptv							0		
n-Propylbenzene ^a	WAS vs. WAS	pptv							0		
Toluene ^a	WAS vs. WAS	pptv	0.93 ± 0.03	0.16 ± 1.1	0.98				21	4	151
3-Ethyltoluene ^a	WAS vs. WAS	pptv							0		
4-Ethyltoluene ^a	WAS vs. WAS	pptv							0		
m-Xylene ^a	WAS vs. WAS	pptv							0		
p-Xylene ^a	WAS vs. WAS	pptv							0		
o-Xylene ^a	WAS vs. WAS	pptv							1		

^a Online files found in VOCs link at <http://www-air.larc.nasa.gov/missions/intex-b/intexb.html> under the Measurement Comparisons: MILAGRO/INTEX-B/IMPEX link.

^b Online files found in halocarbons link at <http://www-air.larc.nasa.gov/missions/intex-b/intexb.html> under the Measurement Comparisons: MILAGRO/INTEX-B/IMPEX link.

^c Online files found in alkyl nitrates link at <http://www-air.larc.nasa.gov/missions/intex-b/intexb.html> under the Measurement Comparisons: MILAGRO/INTEX-B/IMPEX link.

Table 3f. Statistical results of DC-8/C-130 intercomparison. j -values. NOTE: Technique is listed as X (C-130) vs. Y (DC-8).

Species	Technique	Units	Slope	Intercept	R^2	Ratio Percentiles			# Pts	Range	
						25th	50th	75th		Min	Max
$j(\text{O}_3)$	SAFS vs. SAFS	s^{-1}	1.01 ± 0.01	0.00 ± 0.00	0.98				850	2E-5	6E-5
$j(\text{NO}_2)$	SAFS vs. SAFS	s^{-1}	0.93 ± 0.01	0.00 ± 0.00	0.98				867	0.009	0.015

estimates were similar; ODR variance and mse were smaller than that from OLS about 25% of the time. OLS results were significantly better than ODR only 2% of the time, (Boggs et al., 1988). While ODR allows for the possibility of assigning specific uncertainties to each data point, an accurate estimate of measurement uncertainty is not often available on point by point basis. Even when available, this can be complicated when merging measurements of differing integration times. Therefore, in the interest of treating all the intercomparisons uniformly, we use w_{ε_i} and $w_{\delta_i} = 1$. The coefficient of determination, R^2 , is used to indicate the quality of the linear relationship between the paired measurements.

5 Result

5.1 INTEX-B intercomparison

Three types of comparisons were conducted and are presented below: DC-8 to C-130 (Table 3), DC-8 to DC-8 (Table 4), and C-130 to C-130 (Table 5). One hundred and forty parameters were grouped according to chemical similarities and compared. The chemical groups for intercomparison purposes are photochemical precursors and gas phase trac-

ers, photochemical products, photochemical radicals, oxygenated volatile organic carbons (OVOCs), non-methane hydrocarbons (NMHCs) along with halocarbons, alkylnitrates, and organic sulfur compounds, photolysis frequencies, particle microphysical properties, particle chemical composition, and particle scattering and absorption.

As stated previously, when R^2 is greater than or equal to 0.75, the slope and intercept of the regression are given to represent the level of measurement consistency. It is noted here that the intercept should not simply be interpreted as the offset between the instruments. When R^2 is less than 0.75 percentile statistics are given based on the ratio of the data (DC-8/C-130). The resulting statistics are given in the following Table 3a through Table 3i for the DC-8 to C-130 comparison. All analyses are based on the archived final data combined from all three intercomparison flights. No statistical analyses are provided when there are an insufficient number of data points to adequately represent the entire intercomparison periods. Finally, the range (minimum and maximum) is provided as additional information for the reader. In addition to the comparisons listed in Tables 3, 4, and 5, the uncertainties for each instrument can be found in Table 2. The uncertainties were provided in the final data file archive (Current Archive Status link)

Table 3g. Statistical results of DC-8/C-130 intercomparison. Particle microphysical properties. NOTE: Technique is listed as X (C-130) vs. Y (DC-8).

Species	Technique	Units	Slope	Intercept	R^2	Ratio Percentiles			# Pts	Range	
						25th	50th	75th		Min	Max
$N > 3$ nm	CPC	cm^{-3}	1.19 ± 0.00	-188 ± 36	0.93				7908	35	99 831
$N > 10$ nm (05/15)	CPC	cm^{-3}	0.98 ± 0.00	0.73 ± 2.6	0.98				2981	208	3113
$N > 10$ nm (04/17)	CPC	cm^{-3}	2.18 ± 0.01	-191 ± 7	0.94				2623	119	4161
Hot CN (03/19)	CPC	cm^{-3}	0.47 ± 0.0	871 ± 17	0.96				2290	1166	24 823
Hot CN (05/15)	CPC	cm^{-3}	0.94 ± 0.00	-19 ± 2	0.98				3003	70	2842
N_DMA	DMA	cm^{-3}							11		
N_OPC	OPC	cm^{-3}	0.85 ± 0.01	0 ± 0	0.98				149	4	886
N_APS	APS	cm^{-3}	1.81 ± 0.01	-0.14 ± 0.02	0.97				521	0.14	8
Nsub	OPC	cm^{-3}	0.85 ± 0.01	0 ± 0	0.98				149	4	884
Nsuper	OPC	cm^{-3}	1.29 ± 0.03	-0.05 ± 0.02	0.93				149	0.04	2
N_150C_DMA	DMA	cm^{-3}							1		
N_150C_OPC	OPC	cm^{-3}							10		
Nsub_150C	OPC	cm^{-3}							10		
Nsuper_150C	OPC	cm^{-3}							10		
N_300C_DMA	DMA	cm^{-3}							1		
N_300C_OPC	OPC	cm^{-3}							5		
Nsub_300C	OPC	cm^{-3}							5		
Nsuper_300C	OPC	cm^{-3}							5		
N_400C_OPC	OPC	cm^{-3}							10		
Nsub_400C	OPC	cm^{-3}							10		
Nsuper_400C	OPC	cm^{-3}							10		
V_DMA	DMA	$\mu\text{m}^3 \text{cm}^{-3}$							11		
V_OPC	OPC	$\mu\text{m}^3 \text{cm}^{-3}$	0.99 ± 0.01	0.00 ± 0.05	0.98				149	0.06	9
V_APS	APS	$\mu\text{m}^3 \text{cm}^{-3}$	2.62 ± 0.05	-1.4 ± 0.25	0.83				521	0.13	24
Vsub	OPC	$\mu\text{m}^3 \text{cm}^{-3}$	0.92 ± 0.04	0.0 ± 0.0	0.98				149	0.03	6
Vsuper	OPC	$\mu\text{m}^3 \text{cm}^{-3}$	1.14 ± 0.03	0.0 ± 0.0	0.81				149	0.02	3
V_150C_DMA	DMA	$\mu\text{m}^3 \text{cm}^{-3}$							1		
V_150C_OPC	OPC	$\mu\text{m}^3 \text{cm}^{-3}$							10		
Vsub_150C	OPC	$\mu\text{m}^3 \text{cm}^{-3}$							10		
Vsuper_150C	OPC	$\mu\text{m}^3 \text{cm}^{-3}$							10		
V_300C_DMA	DMA	$\mu\text{m}^3 \text{cm}^{-3}$							1		
V_300C_OPC	OPC	$\mu\text{m}^3 \text{cm}^{-3}$							5		
Vsub_300C	OPC	$\mu\text{m}^3 \text{cm}^{-3}$							5		
Vsuper_300C	OPC	$\mu\text{m}^3 \text{cm}^{-3}$							5		
V_400C_OPC	OPC	$\mu\text{m}^3 \text{cm}^{-3}$							10		
Vsub_400C	OPC	$\mu\text{m}^3 \text{cm}^{-3}$							10		
Vsuper_400C	OPC	$\mu\text{m}^3 \text{cm}^{-3}$							10		

Table 3h. Statistical results of DC-8/C-130 intercomparison. Particle chemical composition. NOTE: Technique is listed as X (C-130) vs. Y (DC-8).

Species	Technique	Units	Slope	Intercept	R^2	Ratio Percentiles			# Pts	Range	
						25th	50th	75th		Min	Max
SO_4^{a}	MC vs. AMS	$\mu\text{g m}^{-3}$			0.37	1.03	1.49	2.02	75	0.04	1.5
	MC vs. PILs	$\mu\text{g m}^{-3}$	0.96 ± 0.05	-0.07 ± 0.03	0.89				47	0.04	1.4

^a Further intercomparisons of the AMS with other instruments during INTEX-B have been presented by DeCarlo et al. (2008) and Dunlea et al. (2009).

Table 3i. Statistical results of DC-8/C-130 intercomparison. Particle scattering and absorption. NOTE: Technique is listed as X (C-130) vs. Y (DC-8).

Species	Technique	Units	Slope	Intercept	R^2	Ratio Percentiles			# Pts	Range	
						25th	50th	75th		Min	Max
Scatt 450 nm	TSI Nephelometer	Mm^{-1}	1.01 ± 0.00	-0.18 ± 0.13	0.99				663	2	113
Scatt 550 nm	TSI Nephelometer	Mm^{-1}	1.08 ± 0.00	-0.11 ± 0.10	0.99				754	0.94	83
Scatt 700 nm	TSI Nephelometer	Mm^{-1}	1.11 ± 0.00	-0.61 ± 0.07	0.99				693	1	55
Scattsub 550 nm	RR Nephelometer	Mm^{-1}	1.32 ± 0.01	-0.60 ± 0.11	0.99				652	0.23	67
Abs 470 nm	PSAP	Mm^{-1}	1.09 ± 0.02	-0.02 ± 0.05	0.95				112	0.04	6
Abs 530 nm	PSAP	Mm^{-1}	1.09 ± 0.03	-0.04 ± 0.04	0.94				110	0.03	5
Abs 660 nm	PSAP	Mm^{-1}	1.19 ± 0.03	-0.08 ± 0.04	0.91				98	0.02	4
SSA	N/A	N/A			0.27	0.99	1.00	1.01	104	0.83	0.98

Table 4a. DC-8 intra-platform comparison. Photochemical precursors. NOTE: Technique is listed as X vs. Y.

Species	Technique	Units	Slope	Intercept	R^2	Ratio Percentiles			# Pts	Range	
						25th	50th	75th		Min	Max
H_2O	DLH vs. Cryo	g kg^{-1}	1.04 ± 0.00	-0.07 ± 0.00	0.99				8133	0.003	17

online at the INTEX-B website (<http://www-air.larc.nasa.gov/missions/intex-b/intexb.html>). For cases where uncertainties were available on a point by point basis, the uncertainty was calculated as a percentage of the measurement. The minimum and maximum percentages are given in parentheses and the median is listed outside the parentheses. We present these comparisons and uncertainties without rating the level of agreement. This is a highly subjective task and we leave it to the reader to make that judgment with appropriate consultation with the respective PIs. For an explanation of “Technique”, the reader is referred to the individual PI files located on the INTEX-B website (<http://www-air.larc.nasa.gov/missions/intex-b/intexb.html>) under the Current Archive Status link.

All intercomparison correlation plots can be found online under the Measurement Comparisons: MILAGRO/INTEX-B/IMPEX link at <http://www-air.larc.nasa.gov/missions/intex-b/intexb.html>. The correlation of the combined data from all three flights is in the summary section. Individual timeseries and correlation plots are also available for each intercomparison on 19 March, 17 April, and 15 May 2006.

As described earlier, intra-platform comparisons were also conducted on both the DC-8 and C-130 aircraft for any overlapping measurements. See Table 4a through Table 4c for a complete list of the species, techniques used, and a statistical summary for the DC-8 to DC-8 comparisons. Tables 5a–e provide statistical summary for the C-130 to C-130 comparisons. Since the instruments were located on the same platform, comparison data was not limited to the intercomparison portions of the flights. Data from the entire mission could be included.

5.2 Comparison with ICARTT data

In addition to the intercomparisons made during INTEX-B, we wish to examine the cases where the same comparisons could be made with data from the ICARTT mission and highlight instances where those intercomparisons show significant change. The ICARTT mission was conducted in 2004, a portion of which was INTEX-A (the predecessor to INTEX-B). For a complete description of INTEX-A see Singh et al. (2006). A full listing of the INTEX-A intercomparisons can be found at <http://www-air.larc.nasa.gov/missions/intexna/meas-comparison.htm>. There are three cases where significant change is observed between INTEX-A and INTEX-B; H_2O_2 , PAN, and total PANs. For H_2O_2 the comparison was a DC-8 intra-platform comparison between CIT CIMS and URI EFD during INTEX-A (Fig. 4a) while for INTEX-B, CIT CIMS was on the C-130 and URI EFD on the DC-8 (Fig. 4b). The INTEX-A comparison included significantly more data pairs and covered a wider range of values since both instruments were on the same aircraft and all mission data could be used. During INTEX-B, R^2 is much improved (0.92 in INTEX-B vs. 0.77 during INTEX-A) however the slope of the regression was better during INTEX-A (1.01 for INTEX-A vs. 1.24 for INTEX-B). This could be due to the smaller amount of data during INTEX-B as well as the smaller dynamic range for the INTEX-B intercomparison measurements.

For PAN, the same instruments were used for both missions ARC PANAK (or dual GC) on the DC-8 for both INTEX-A and INTEX-B; NCAR CIGAR on the NOAA WP-3D for INTEX-A and on the C-130 for INTEX-B). In

Table 4b. DC-8 intra-platform comparison. Photochemical products. NOTE: Technique is listed as X vs. Y.

Species	Technique	Units	Slope	Intercept	R^2	Ratio Percentiles			# Pts	Range	
						25th	50th	75th		Min	Max
CH ₂ O	TDL vs. EFD	pptv	0.83 ± 0.01	-12 ± 8	0.88				2119	LOD	18 830
H ₂ O ₂	ACCD vs. EFD	pptv			0.67	0.56	0.80	1.07	1962	27	9899
HNO ₃	TDLIF vs. MC	pptv	0.91 ± 0.01	-28 ± 4	0.84				2270	3	7530

Table 4c. DC-8 intra-platform comparison. j -values. NOTE: Technique is listed as X vs. Y.

Species	Technique	Units	Slope	Intercept	R^2	Ratio Percentiles			# Pts	Range	
						25th	50th	75th		Min	Max
$j(\text{NO}_2)$	SAFS vs. Filt. Rad.	s ⁻¹	0.96 ± 0.00	0.00 ± 0.00	0.99				6846	LOD	0.02

Table 5a. C-130 intra-platform comparison. Gas phase tracers. NOTE: Technique is listed as X vs. Y.

Species	Technique	Units	Slope	Intercept	R^2	Ratio Percentiles			# Pts	Range	
						25th	50th	75th		Min	Max
SO ₂	CIMS vs. UVF ^a	ppbv	0.76 ± 0.00	0.24 ± 0.03	0.90				5799	LOD	392
SO ₂	CIMS vs. UVF ^b	ppbv	0.87 ± 0.00	0.07 ± 0.02	0.91				5854	LOD	100
CH ₃ CN	PTRMS vs. TOGA	pptv			0.40	0.71	0.96	1.33	1575	LOD	5.13

^a All data. ^b SO₂ ≤ 100 ppbv.

Table 5b. C-130 intra-platform comparison. Photochemical products. NOTE: Technique is listed as X vs. Y.

Species	Technique	Units	Slope	Intercept	R^2	Ratio Percentiles			# Pts	Range	
						25th	50th	75th		Min	Max
Acetic Acid	CIMS vs. PTRMS	pptv			0.55	0.40	0.76	1.36	3909	LOD	10

Table 5c. C-130 intra-platform comparison. Oxygenated volatile organic carbons. NOTE: Technique is listed as X vs. Y.

Species	Technique	Units	Slope	Intercept	R^2	Ratio Percentiles			# Pts	Range	
						25th	50th	75th		Min	Max
Acetaldehyde	PTRMS vs. TOGA	pptv			0.50	0.68	1.24	2.58	1511	LOD	11.3
Methanol	PTRMS vs. TOGA	pptv			0.72	0.56	0.83	1.24	3442	0.02	37

this case, the INTEX-A intercomparison was better than the INTEX-B intercomparison. During INTEX-B, $R^2 = 0.77$ and slope = 1.68, while for INTEX-A $R^2 = 0.82$ and slope = 0.99. During INTEX-B most data was below 500 pptv (19 March flight had values up to about 1400 pptv). For INTEX-A most data was also below 500 pptv with a few points up to about 750 pptv. During INTEX-B the higher values skewed the

regression slope. Removing the 5 points where either the DC-8 or C-130 value is above 500 pptv increases R^2 slightly to 0.79 and decreases the slope to 1.23.

The total PANs intercomparisons for INTEX-A and INTEX-B included the same instruments for both missions, with instruments on separate planes for both missions. Both intercomparisons are generally consistent (INTEX-B

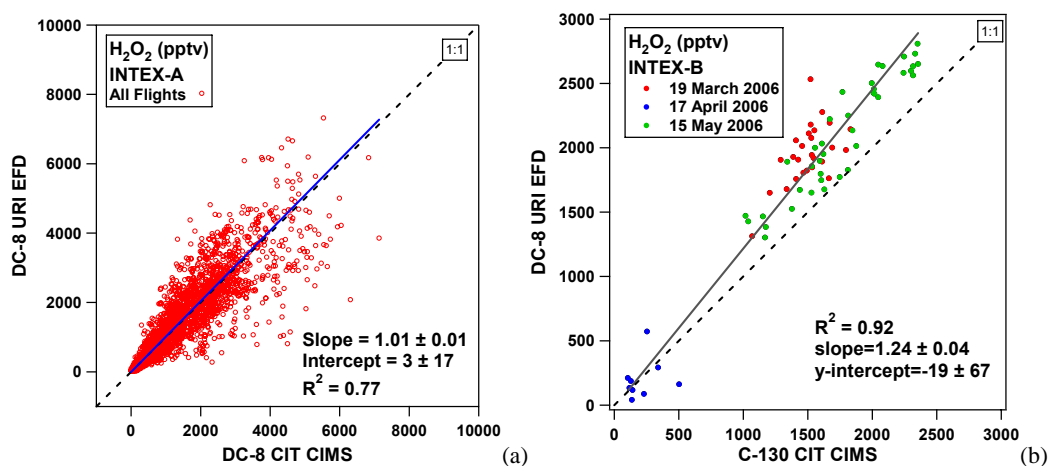


Fig. 4. (a) Scatter plot and orthogonal distance regression for the DC-8 CIMS and EFD H_2O_2 intercomparison of all INTEX-A flights. (b) Scatter plot and orthogonal distance regression for the DC-8 and C-130 H_2O_2 INTEX-B intercomparisons on 19 March (red), 17 April (blue), and 15 May (green) 2006.

Table 5d. C-130 intra-platform comparison. Nonmethane hydrocarbons, halocarbons, and organic sulfur compounds. NOTE: Technique is listed as X vs. Y.

Species	Technique	Units	Slope	Intercept	R^2	Ratio Percentiles			# Pts	Range	
						25th	50th	75th		Min	Max
DMS	TOGA vs. WAS	pptv							44		
CHCl_3^a	TOGA vs. WAS	pptv	1.25 ± 0.03	0.20 ± 0.22	0.86				388	5	14
CHCl_3^b	TOGA vs. WAS	pptv			0.47	0.74	0.79	0.85	256	5	17
CH_3Cl	TOGA vs. WAS	pptv			0.02	0.96	1.05	1.11	287	281	1509
i-Butane	TOGA vs. WAS	pptv	1.06 ± 0.01	0.62 ± 3.35	0.93				455	2	608
n-Butane	TOGA vs. WAS	pptv	0.85 ± 0.01	22.3 ± 7.3	0.94				571	4	1634
i-Pentane	TOGA vs. WAS	pptv	1.19 ± 0.01	13.3 ± 3.1	0.95				523	1	938
n-Pentane	TOGA vs. WAS	pptv	0.87 ± 0.01	4 ± 2	0.93				471	2	436
Isoprene	TOGA vs. WAS	pptv							1		
Benzene	TOGA vs. WAS	pptv	1.26 ± 0.02	-16.4 ± 1.7	0.91				664	8	336
Toluene	TOGA vs. WAS	pptv	1.19 ± 0.02	1.7 ± 9.1	0.79				440	0.44	1112
o-Xylene	TOGA vs. WAS	pptv							91		

^a Pacific Phase.

^b Mexico City Phase.

$R^2 = 0.94$, slope = 1.35; INTEX-A $R^2 = 0.87$, slope = 0.95). R^2 was better for INTEX-B while the slope of the regression was better for INTEX-A. The range of values during INTEX-B is almost twice the range during INTEX-A. Again, during INTEX-B a few high values from the 19 March flight skew the slope of the regression. By removing the seven points above 1000 pptv, the slope is reduced to 1.15, (R^2 is also reduced to a value of 0.84).

6 Summary

This paper provides a comprehensive overview and a record of measurement consistency of approximately 140 inter-comparisons of data acquired during the INTEX-B airborne

field campaign conducted in the spring of 2006. A complete set of timeseries and correlation figures can be found at <http://www-air.larc.nasa.gov/missions/intex-b/intexb.html> under the Measurement Comparisons: MILAGRO/INTEX-B/IMPEx link. For interpretation and most effective use of these results, the reader is strongly urged to consult with the instrument PIs. We leave it to the reader to determine the level of consistency between the instruments compared. This should be done not only with the statistical analyses provided in Tables 3, 4, and 5, but also in consideration of the uncertainties in Table 2, keeping in mind that even when measurements are technically consistent within the PI reported uncertainties, significant differences between the measurements can still exist if the uncertainties are large. In addition, future instrument work may benefit from this assessment.

Table 5e C-130 intra-platform comparison. Particle chemical composition. NOTE: Technique is listed as X vs. Y.

Species	Technique	Units	Slope	Intercept	R^2	Ratio Percentiles			# Pts	Range	
						25th	50th	75th		Min	Max
SO ₄ ^{=a}	PILS vs. AMS	µg m ⁻³			0.45	0.50	0.88	1.50	3669	0.02	15.8
NO ₃ ^{-a}	PILS vs. AMS	µg m ⁻³	1.54 ± 0.03	0.15 ± 0.10	0.88				410	0.02	25
NH ₄ ^{3+a}	PILS vs. AMS	µg m ⁻³	0.78 ± 0.01	0.02 ± 0.02	0.75				2496	0.1	9.4

^a Further intercomparisons of the AMS with other instruments during INTEX-B have been presented by DeCarlo et al. (2008) and Dunlea et al. (2009).

Appendix A

Acronyms and abbreviations.

Abs 470 nm	Aerosol absorption coefficient at 470 nm	Hot CN	Condensation nuclei with heated inlet to 300 °C
Abs 530 nm	Aerosol absorption coefficient at 530 nm	ICARTT	International Consortium for Atmospheric Research on Transport and Transformation
Abs 660 nm	Aerosol absorption coefficient at 660 nm	IMPEX	Intercontinental and Mega-city Pollution Experiment
ACCD	Aqueous Collection Chemiluminescence Detection	INTEX-A	Intercontinental Chemical and Transport Experiment – A
ACD	Atmospheric Chemistry Division	INTEX-B	Intercontinental Chemical and Transport Experiment – B
AMS	Aerodyne High-Resolution Aerosol Mass Spectrometer	INTEX-NA	Intercontinental Chemical and Transport Experiment – North America
APS	Aerodynamic Particle Sizer	ITOP	Intercontinental Transport of Ozone and Precursors
ARC	Ames Research Center	LaRC	Langley Research Center
ARIM	Atmospheric Radiation Investigation and Measurements	LOD	Limit of Detection
ATHOS	Airborne Tropospheric Hydrogen Oxides Sensor	MC	Mist Chamber
CIGAR	CIMS Instrument by Georgia Tech and NCAR	MCWG	Measurement Comparison Working Group
CIMS	Chemical Ionization Mass Spectrometry	MEK	Methyl ethyl ketone
CIT	California Institute of Technology	MILAGRO	Mega-city Initiative: Local and Global Research Observations
CITE	Chemical Instrumentation Test and Evaluation	MBL	Marine boundary layer
CLD	Chemiluminescence Detector	N_150C_DMA	Aerosol number density, inlet heated to 150 °C, measured with differential mobility analyzer
CN	Condensation nuclei	N_150C_OPC	Aerosol number density, inlet heated to 150 °C, measured with optical particle counter
CPC	Condensation Particle Counter	N_300C_DMA	Aerosol number density, inlet heated to 300 °C, measured with differential mobility analyzer
Cryo	Cryo-hygrometer	N_300C_OPC	Aerosol number density, inlet heated to 300 °C, measured with optical particle counter
DACOM	Differential Absorption CO Measurement	N_400C_OPC	Aerosol number density, inlet heated to 400 °C, measured with optical particle counter
DFG	Difference Frequency Generation Absorption Spectrometer	N_APS	Aerosol number density, measured with aerodynamic particle sizer
DLH	Diode Laser Hygrometer	N_DMA	Aerosol number density, measured with differential mobility analyzer
DMA	Differential Mobility Analyzer		
DMS	Dimethyl sulfide		
EFD	Enzyme Fluorescence Detection		
FT	Free troposphere		
GIT	Georgia Institute of Technology		
HCN	Hydrogen cyanide		

N OPC	Aerosol number density, measured with optical particle counter	Scatt 700 nm	Aerosol scattering coefficient at 700 nm
NASA	National Aeronautics and Space Administration	Scattsub 550 nm	Submicron aerosol scattering coefficient at 550 nm
NCAR	National Center for Atmospheric Research	SSA	Single Scattering Albedo
NEAQS – ITCT 2004	New England Air Quality Study – Intercontinental Transport and Chemical Transformation, 2004	TD-LIF	Thermal dissociation-laser induced fluorescence
NMHCs	Non-methane hydrocarbons	TDL	Tunable Diode Laser Absorption Spectrometer
NOAA	National Oceanic and Atmospheric Administration	TOGA	Trace Organic Gas Analyzer
NO _y	Reactive nitrogen	TRACE-P	Transport and Chemical Evolution over the Pacific
NSERC	National Suborbital Education and Research Center	TSI Nephelometer	TSI, Inc. nephelometer
NSF	National Science Foundation	UC	University of California
Nsub	Submicron aerosol number density	UCI	University of California, Irvine
Nsub_150C	Submicron aerosol number density, inlet heated to 150 °C	UND	University of North Dakota
Nsub_300C	Submicron aerosol number density, inlet heated to 300 °C	UNH	University of New Hampshire
Nsub_400C	Submicron aerosol number density, inlet heated to 400 °C	URI	University of Rhode Island
Nsuper	Supermicron aerosol number density	USNA	United States Naval Academy
Nsuper_150C	Supermicron aerosol number density, inlet heated to 150 °C	V APS	Aerosol volume density, measured with aerodynamic particle sizer
Nsuper_300C	Supermicron aerosol number density, inlet heated to 300 °C	V_DMA	Aerosol volume density, measured with differential mobility analyzer
Nsuper_400C	Supermicron aerosol number density, inlet heated to 400 °C	V OPC	Aerosol volume density, measured with optical particle counter
ODR	Orthogonal Distance Regression	V_150C_DMA	Aerosol volume density, inlet heated to 150 °C, measured with differential mobility analyzer
OLS	Ordinary Least Squares	V_150C OPC	Aerosol volume density, inlet heated to 150 °C, measured with optical particle counter
OPC	Optical Particle Counter	V_300C_DMA	Aerosol volume density, inlet heated to 300 °C, measured with differential mobility analyzer
OVOC	Oxygenated Volatile Organic Carbon	V_300C OPC	Aerosol volume density, inlet heated to 300 °C, measured with optical particle counter
PAN	Peroxyacetyl Nitrate	V_400C OPC	Aerosol volume density, inlet heated to 400 °C, measured with optical particle counter
PANAK	PAN/Aldehyde/Ketone Photo Ionization Detector		
PILS	Particle-Into-Liquid Sampler	UVF	Ultra-violet fluorescence
PSAP	Particle Soot Absorption Photometer	Vsub	Submicron aerosol volume density
PTRMS	Proton Transfer Reaction Mass Spectrometry	Vsub_150C	Submicron aerosol volume density, inlet heated to 150 °C
RAF	Research Aviation Facility	Vsub_300C	Submicron aerosol volume density, inlet heated to 300 °C
RR Nephelometer	Radiance Research nephelometer	Vsub_400C	Submicron aerosol volume density, inlet heated to 400 °C
SAFS	Scanning actinic flux spectroradiometer	Vsuper	Supermicron aerosol volume density
Scatt 450 nm	Aerosol scattering coefficient at 450 nm		
Scatt 550 nm	Aerosol scattering coefficient at 550 nm		

Vsuper_150C	Supermicron aerosol volume density, inlet heated to 150 °C
Vsuper_300C	Supermicron aerosol volume density, inlet heated to 300 °C
Vsuper_400C	Supermicron aerosol volume density, inlet heated to 400 °C
WAS	Whole Air Sampling

Acknowledgements. The authors wish to thank the National Aeronautics and Space Administration (NASA) Tropospheric Chemistry (TCP) and Making Earth System data records for Use in Research Environments (MEASURE) Programs for their support of the measurements and intercomparisons presented in this paper. We also thank the National Science Foundation Atmospheric Chemistry Program for support of this study. We would like to thank the pilots and crew of the NASA DC-8 and the NSF C-130 and the INTEX-B and IMPEX/MILAGRO science teams for contributing to the success of this study. Finally, we thank Ms. Amy Thornhill for her assistance in acquiring additional uncertainty information from principal investigators.

Edited by: D. Heard

References

- Bahreini, R., Evans, B., Middlebrook, A. M., Warneke, C., de Gouw, J. A., De Carlo, P. F., Jimenez, J. L., Brock, C. A., Neuman, J. A., Ryerson, T. B., Stark, H., Atlas, E., Brioude, J., Fried, A., Holloway, J. S., Peischl, J., Richter, D., Walega, J., Weibring, P., Wollny, A. G., and Fehsenfeld, F. C.: Organic aerosol formation in urban and industrial plumes near Houston and Dallas, Texas, *J. Geophys. Res.*, 114, DF00F16, doi:10.1029/2008JD011493, 2009.
- Beck, S. M., Bendura, R. J., McDougal, D. S., Hoell, J. M., Gregory, G. L., Curfman, H. J., Davis, D. D., Bradshaw, J., Rodgers, M. O., Wang, C. C., Davis, L. I., Campbell, M. J., Torres, A. L., Carroll, M. A., Ridley, B. A., Sachse, G. W., Hill, G. F., Condon, E. P., and Rasmussen, R. A.: Operational Overview of NASA GTE/CITE 1 Airborne Instrument Intercomparisons: Carbon Monoxide, Nitric Oxide, and Hydroxyl Instrumentation, *J. Geophys. Res.*, 92, 1977–1985, 1987.
- Boggs, P. T., Spiegelman, C. H., Donaldson, J. R., and Schnabel, R. B.: A computational examination of orthogonal distance regression, *J. Econometr.*, 38, 169–201, 1988.
- DeCarlo, P. F., Dunlea, E. J., Kimmel, J. R., Aiken, A. C., Sueper, D., Crouse, J., Wennberg, P. O., Emmons, L., Shinozuka, Y., Clarke, A., Zhou, J., Tomlinson, J., Collins, D. R., Knapp, D., Weinheimer, A. J., Montzka, D. D., Campos, T., and Jimenez, J. L.: Fast airborne aerosol size and chemistry measurements above Mexico City and Central Mexico during the MILAGRO campaign, *Atmos. Chem. Phys.*, 8, 4027–4048, doi:10.5194/acp-8-4027-2008, 2008.
- Dunlea, E. J., DeCarlo, P. F., Aiken, A. C., Kimmel, J. R., Peltier, R. E., Weber, R. J., Tomlinson, J., Collins, D. R., Shinozuka, Y., McNaughton, C. S., Howell, S. G., Clarke, A. D., Emmons, L. K., Apel, E. C., Pfister, G. G., van Donkelaar, A., Martin, R. V., Millet, D. B., Heald, C. L., and Jimenez, J. L.: Evolution of Asian aerosols during transpacific transport in INTEX-B, *Atmos. Chem. Phys.*, 9, 7257–7287, doi:10.5194/acp-9-7257-2009, 2009.
- Eisele, F. L., Mauldin, L., Cantrell, C., Zondlo, M., Apel, E., Fried, A., Walega, J., Shetter, R., Lefer, B., Flocke, F., Weinheimer, A., Avery, M., Vay, S., Sachse, G., Podolske, J., Diskin, G., Barrick, J. D., Singh, H. B., Brune, W., Harder, H., Martinez, M., Bandy, A., Thornton, D., Heikes, B., Kondo, Y., Reimer, D., Sandholm, S., Tan, D., Talbot, R., and Dibb, J.: Summary of measurement intercomparisons during TRACE-P, *J. Geophys. Res.*, 108, 8791, doi:10.1029/2002JD003167, 2003.
- Gregory, G. L., Hoell, J. M., Beck, S. M., McDougal, D. S., Meyers, J. A., and Bruton, D. B.: Operational Overview of Wallops Island Instrument Intercomparison: Carbon Monoxide, Nitric Oxide, and Hydroxyl Instrumentation, *J. Geophys. Res.*, 90, 12808–12818, 1985.
- Gregory, G. L., Davis, D. D., Beltz, N., Bandy, A. R., Ferek, R. J., and Thornton, D. C.: An Intercomparison of Aircraft Instrumentation for Tropospheric Measurements of Sulfur Dioxide, *J. Geophys. Res.*, 98, 23325–23352, 1993a.
- Gregory, G. L., Davis, D. D., Thornton, D. C., Johnson, J. E., Bandy, A. R., Saltzman, E. S., Andreae, M. O., and Barrick, J. D.: An Intercomparison of Aircraft Instrumentation for Tropospheric Measurements of Carbonyl Sulfide, Hydrogen Sulfide, and Carbon Disulfide, *J. Geophys. Res.*, 98, 23353–23372, 1993b.
- Gregory, G. L., Warren, L. S., Davis, D. D., Andreae, M. O., Bandy, A. R., Ferek, R. J., Johnson, J. E., Saltzman, E. S., and Cooper, D. J.: An Intercomparison of Instrumentation for Tropospheric Measurements of Dimethyl Sulfide: Aircraft Results for Concentrations at the Parts-Per-Trillion Level, *J. Geophys. Res.*, 98, 23373–23388, 1993c.
- Hoell, J. M., Gregory, G. L., Carroll, M. A., McFarland, M., Ridley, B. A., Davis, D. D., Bradshaw, J., Rodgers, M. O., Torres, A. L., Sachse, G. W., Hill, G. F., Condon, E. P., Rasmussen, R. A., Campbell, M. C., Farmer, J. C., Sheppard, J. C., Wang, C. C., and Davis, L. I.: An Intercomparison of Carbon Monoxide, Nitric Oxide, and Hydroxyl Measurement Techniques: Overview of Results, *J. Geophys. Res.*, 89, 11819–11825, 1984.
- Hoell, J. M., Gregory, G. L., McDougal, D. S., Carroll, M. A., McFarland, M., Ridley, B. A., Davis, D. D., Bradshaw, J., Rodgers, M. O., and Torres, A. L.: An Intercomparison of Nitric Oxide Measurement Techniques, *J. Geophys. Res.*, 90, 12843–12852, 1985a.
- Hoell, J. M., Gregory, G. L., McDougal, D. S., Sachse, G. W., Hill, G. F., Condon, E. P., and Rasmussen, R. A.: An Intercomparison of Carbon Monoxide Measurement Techniques, *J. Geophys. Res.*, 90, 12881–12890, 1985b.
- Hoell, J. M., Albritton, D. L., Gregory, G. L., McNeal, R. J., Beck, S. M., Bendura, R. J., and Drewery, J. W.: Operational Overview of NASA GTE/CITE 2 Airborne Instrument Intercomparisons: Nitrogen Dioxide, Nitric Acid, and Peroxyacetyl Nitrate, *J. Geophys. Res.*, 95, 10047–10057, 1990.
- Hoell, J. M., Davis, D. D., Gregory, G. L., McNeal, R. J., Bendura, R. J., Drewery, J. W., Barrick, J. D., Kirchhoff, V. W. J. H., Motta, A. G., Navarro, R. L., Dorko, W. D., and Owen, D. W.: Operational Overview of the NASA GTE/CITE 3 Airborne Instrument Intercomparisons for Sulfur Dioxide, Hydrogen Sulfide, Carbonyl Sulfide, Dimethyl Sulfide, and Carbon Disulfide, *J. Geophys. Res.*, 98, 23291–23304, 1993.

- Singh, H. B., Brune, W. H., Crawford, J. H., Jacob, D. J., and Russell, P. B.: Overview of the summer 2004 Intercontinental Chemical Transport Experiment- North America (INTEX-A), *J. Geophys. Res.*, 111, D24S01, doi:10.1029/2006JD007905, 2006.
- Singh, H. B., Brune, W. H., Crawford, J. H., Flocke, F., and Jacob, D. J.: Chemistry and transport of pollution over the Gulf of Mexico and the Pacific: spring 2006 INTEX-B campaign overview and first results, *Atmos. Chem. Phys.*, 9, 2301–2318, doi:10.5194/acp-9-2301-2009, 2009.
- Zwolak, J. W., Boggs, P. T., and Watson, L. T.: Algorithm 869: ODRPACK95: A weighted orthogonal distance regression code with bound constraints, <http://doi.acm.org/10.1145/1268776.1268782>, last access: 3 January 2011, *ACM Trans. Math. Softw.*, 33(4), 27, doi:10.1145/1268776.1268782, 2007.